# INTERNATIONAL SOCIETY FOR SOIL MECHANICS AND GEOTECHNICAL ENGINEERING



This paper was downloaded from the Online Library of the International Society for Soil Mechanics and Geotechnical Engineering (ISSMGE). The library is available here:

https://www.issmge.org/publications/online-library

This is an open-access database that archives thousands of papers published under the Auspices of the ISSMGE and maintained by the Innovation and Development Committee of ISSMGE.

# Parameter identification for effective stress analysis from a multi-stage cyclic loading test



Koji Ichii Kansai University, Takatsuki, Osaka, Japan Toshiki Murakami Hiroshima University, Higashi-hiroshima, Hiroshima, Japan Takeko Mikami Maeda Co. Ltd., Tokyo, Tokyo, Japan

#### **ABSTRACT**

In this paper, we challenged parameter calibration of an effective stress analysis from multi-stage cyclic loading test result. Different from a standard multi-stage cyclic loading test as indicated in JGS 0543-2009 "Method for Cyclic Torsional Shear Test on Hollow Cylindrical Specimens to Determine Deformation Properties of Soils", pore water pressure during the test was recorded in the test. The recorded pore water pressure clarified the drawback of the multi-stage test such as the densification of the specimen due to the drainage between the loading stages. With the recorded pore water pressure increase in the test, parameters for an effective stress analysis program: FLIP ROSE (strain space multi-spring model) can be obtained. The validation of the obtained parameter sets was examined by the comparison of liquefaction resistance curve by the test and analysis. The example of parameter identification in this paper may be a useful reference in the practice, especially in the case with insufficient number of undisturbed in-situ samples to obtain the liquefaction resistance curve.

# 1 INTRODUCTION

As a tool of seismic performance verification in PBD, various types of effective stress model has been proposed (i.e., Dafalias and Manzari 2004; Boulanger and Ziotopoulou 2015, Fukutake 1990; lai et al. 2011). Some of them are implemented in 2D or 3D / FEM or FDM, and they work very well in design practice. However, one of the difficulties in the application of these advanced models is the parameter identification.

Various kind of test results are necessary for the implementation of effective stress analysis. The necessity of these test results can be a barrier in the practical use of advanced model.

Furthermore, the parameters for the effective stress analysis are often given by the calibration analysis on liquefaction tests. However, several pieces of specimen with uniform characteristics/quality are necessary for liquefaction test. The difference in characteristics or quality of specimen may result an irregularity in obtained liquefaction resistance curve.

The appropriate parameter identification scheme is necessary to implement effective stress analyses in PBD. Thus, research on parameter identification scheme is quite essential in PBD.

In this paper, an application of multi-stage cyclic loading test of single specimen for parameter calibration of an effective stress analysis was examined. With the recorded pore water pressure, parameters for an effective stress analysis, FLIP ROSE (strain space multi-spring model) can be obtained. The validation of the obtained parameter sets were examined by the comparison of liquefaction resistance curve by the test and analysis.

# 2 MULTI-STAGE CYCLIC LOADING TEST

Multi-stage cyclic loading test is a test to obtain dynamic properties of soil. The test results are often summarized as shear modulus and damping factor depending on strain level. Figure 1 is an example of the results of multistage cyclic loading test to obtain dynamic soil property.

These results are used in equivalent linear analysis such as SHAKE (Shnabel et al. 1972). In other words, the test scheme of multi-stage cyclic loading test is designed for the application of seismic response analysis by equivalent linear method. However, these test results are not enough to conduct effective stress analysis.

Table 1 shows the parameters and in-situ or laboratory tests used in the parameter identification process for a model used in FLIP ROSE. This model is an old-type dilatancy model with multiple shear mechanism model (lai et al. 1992) and different from the latest "Cocktail-glass model" (lai et al. 2011).

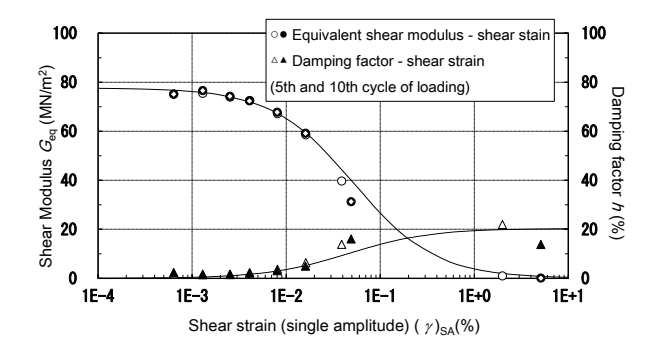


Figure 1. An example of the test results from multi-stage cyclic loading test (Toyoura sand, Dr = 50 %)

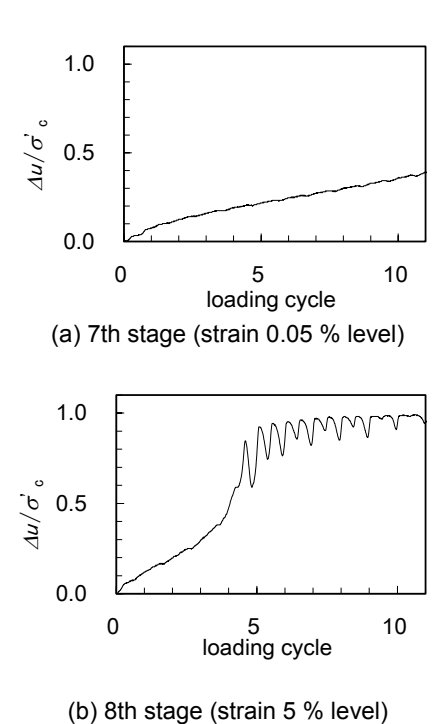
Table 1. Example of test list for parameter identification in a model (lai et al. 1992) in FLIP ROSE

Parameter type	Parameter	Test			
Physical property	Wet density ρt	Test of a sample or in-situ measurement			
	Porosity n	Test of a sample			
Dynamic property	Reference confining stress	Calculate as the in-situ confining stress from the densities of soil layers			
	Shear modulus for small strain $G_{ma}$	Given by in-situ P-S logging results.			
	Bulk modulus K <sub>ma</sub>	Calculate from shear modulus and Poisson's ratio of soil skeleton (assume 0.33)			
	Friction angle $\phi_{\rm f}$	CD test or CUB test (sometimes from stress path in liquefaction test)			
	Cohesion c'	Assume zero for sand. Obtain from test results for clay.			
	Maximum damping factor $h_{max}$	Given from multi-stage cyclic loading test for dynamic soil property			
	Stress level for steady state $S_{us}$	Undrained shearing test for large strain level			
Dilatancy	Phase transformation angle $\phi_p$	Obtained from stress path in liquefaction test (or often assume a constant value: 28 deg.)			
	Liquefaction parameters w <sub>1</sub> , p <sub>1</sub> , p <sub>2</sub> , c <sub>1</sub> , s <sub>1</sub>	Trial and error procedure to simulate liquefaction test results.			

As shown in Table 1, most of the parameters for dilatancy characteristics are obtained by a liquefaction test. Dynamic soil property results from multi-stage cyclic loading test is only for the identification of damping factor. Since the multi-stage cyclic loading test has a long history in practice and there are a large amount of data and experiences of the test, we would like to use the test results from multi-stage cyclic loading test more effectively.

For example, Figure 2 shows the pore water pressure generation in multi-stage cyclic loading test. In this test scheme (JGS 0543-2009 "Method for Cyclic Torsional Shear Test on Hollow Cylindrical Specimens to Determine Deformation Properties of Soils"), drainage shall be done between loading stages while undrained condition shall be maintained in each loading stage. Thus, increases of the excess pore water pressure are observed in the stage with large strain level. This fact implies that the observed

pore water pressure generation can be a useful information in parameter setting for dilatancy model.



(a) an ange (an am a va aran,

Figure 2. An example of pore water pressure increase in multi stage cyclic loading test

# 3 PARAMETER SETTING

# 3.1 Multi stage cyclic loading test data

Four cases of multi stage cyclic loading test data were prepared. The test procedure followed the Japanese standard scheme for hollow cylinder specimen (JGS 0543-2009 "Method for Cyclic Torsional Shear Test on Hollow Cylindrical Specimens to Determine Deformation Properties of Soils"). Toyoura sand of Dr = 50 % and 80 % were tested both by stress control and by strain control scheme. The test cases are summarized in Table 2. In JGS 0543-2009, measurement of pore water pressure is not mandatory since the main purpose of the test is to determine the dynamic soil properties. However, in these test, pore water pressure were also recorded.

# 3.2 Shear modulus (small strain level): G<sub>ma</sub>

In practice, shear modulus (shear modulus in small strain level) shall be obtained from the in-situ shear wave velocity measurement (PS logging). However, the specimen for the tests in this study are reconstituted samples and it is impossible to prepare the values of insitu measurement. Thus, shear modulus for small strain level:  $G_{ma}$  was obtained from the test result of the 1st stage. Note notation  $G_{ma}$  is used for  $G_{max}$  at the specified reference confining stress of  $\sigma_{max}$ . Figure 3 shows the

stress-strain relationship in case 1. From the 1st half cycle of loading, shear modulus were determined. The strain level for this 1st half cycle is approx.  $6.0 \times 10^{-6}$ . As shown in Figure 3, stress-strain relationship is almost linear and the modulus is almost same with the shear modulus in 10th cycle when the drift of the origin is disregarded. The reference confining stress for this shear modulus is given as the initial confining effective stress in the test.

# 3.3 Friction angle

In practice, friction angle of the soil shall be obtained from CD tests or CUB tests results. However, the determination of friction angle from the effective stress path was challenged. Figure 4 shows the effective stress path in the test, and the friction angle was determined by the envelope of the stress path.

The determination of friction angle is only possible by the results in later stages. In beginning stages, the stress path was not close to the failure line. It implies that the densification of the specimen between stages may cause an error in the estimated friction angle. The small offsets or drifts in the measurements also made it difficult.

# 3.4 Phase transformation angle

As same as the friction angle, the phase transformation angle  $\phi_p$  can be determined by the effective stress path. Figure 5 shows the determination of the phase transformation angle. Although the points of inflection in effective stress path seems to be fluctuated, the first point of inflection in the path was used for the determination.

Table 2. Test cases in this study

Cases	<i>D</i> r	Test procedure
1	50	stress controlled
2	50	strain controlled
3	80	stress controlled
4	80	strain controlled

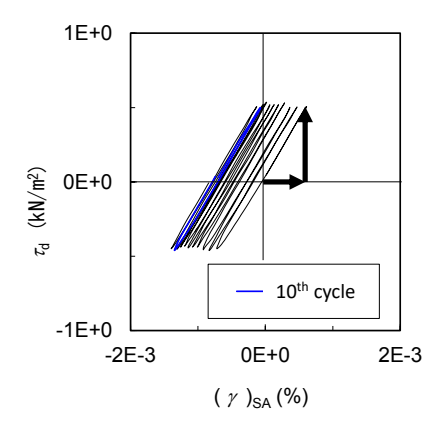


Figure 3. Shear modulus determination from the stress-strain relationship in the 1st stage (case 1)

#### 3.5 Parameter for the threshold strain

For clean sand, the threshold strain for pore water pressure generation were given as 0.01 % (Dobry et al. 1982; Vucetic 1994). This information can be used to determine some part of the parameters.

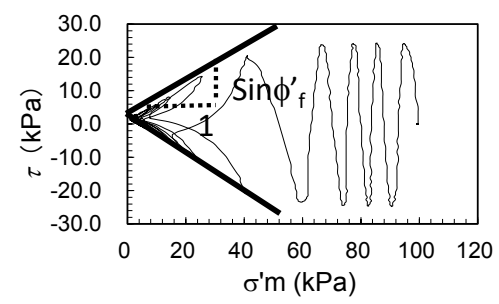


Figure 4. Friction angle determination from the effective stress path in the 8th stage (case 1)

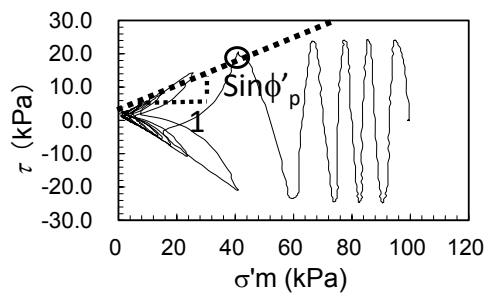


Figure 5. Phase transformation angle determination from the effective stress path in the 8th stage (case 1)

For example, the increase in pore water pressure (decrease in effective stress) is given by the sum of plastic shear work in the model. And in the model, a parameter:  $c_1$  was used to adjust the amount of elastic shear work, which shall be subtracted from total shear work to obtain the plastic portion of the shear work. Thus, the condition where no pore water pressure generation in small increment of strain is.

$$\tau \Delta \gamma - c_1 \tau \frac{\Delta \gamma}{G_0} \le 0$$
 [1].

Then,

$$c_1 \ge G_0 \frac{\Delta \gamma}{\Delta \tau}$$
 [2].

Since the stress-strain relationship is assumed to follow the hyperbolic relationship, stress state on the backbone curve is,

$$\tau = \frac{\gamma G_0}{1 + \gamma G_0 / \tau_f}$$
 [3].

Thus,

$$\gamma = \frac{\tau}{G_0 \left( 1 - \tau / \tau_f \right)}$$
 [4].

From the differentiation of Eq. 4,

$$\frac{\Delta \gamma}{\Delta \tau} = \frac{1}{G_0 (1 - \tau / \tau_f)^2}$$
 [5].

Thus, as same as Uemura et al. (1992),

$$c_1 \ge \frac{1}{\left(1 - \tau/\tau_f\right)^2} = \frac{1}{\left(1 - \left(\tau/\sigma_m'\right)/\sin\phi_f\right)^2}$$
 [6].

The Eq. 6 shows the lower bound for the parameter  $c_1$ . The stress level  $\tau_{\text{lim}}$  for threshold shear strain  $\gamma_{\text{lim}}$  is,

$$\tau_{\lim} = \frac{\gamma_{\lim} G_0}{1 + \gamma_{\lim} G_0 / \tau_f}$$
 [7]

or giving shear modulus G for 0.01 % strain and

$$\tau_{\rm lim} = G_{0.01\%} \gamma_{\rm lim}$$
 [8].

Thus, the lower bound for the parameter  $c_1$  can be given by substituting the value from Eq. 7 or Eq. 8 into the shear stress in Eq. 6. This lower bound may be the first estimation in the parameter determination.

# 3.6 Parameters for pore water generation

In this model, the pore water pressure generation (decrease in effective stress) is modeled by the accumulated plastic shear work as shown in Figure 6. In Figure 6, liquefaction front parameter  $S_0$  is the index representing the effective stress ratio of the soil under no shear stress condition. Although the stress state of the soil depends on the current shear stress level due to the effect of dilatancy (cyclic mobility), the effective stress in case of no shear stress decreases with increasing in plastic shear work. The speed of the effective stress reduction is controlled by parameter  $p_1$  (for first half phase) and  $p_2$  (for last half phase), while overall liquefaction resistance is controlled by  $w_1$ . Here, parameter  $w_1$  is given as the total plastic shear work to reach the stress state so that 40 % of initial effective confining stress remained. The parameter S<sub>1</sub> is given as the ultimate value in the model, introducing small value of residual effective stress to maintain the numerical stability even in the extensive liquefaction.

In order to give these parameters:  $p_1$ ,  $p_2$ ,  $w_1$ ,  $S_1$ , the relationship between the effective stress ratio and plastic shear work are calculated. Figure 7 shows the result for 8th stage in case 1. The fluctuation of effective stress ratio is due to the cyclic mobility of the sand (effect of positive dilatancy due to the increase in shear stress). If we can disregard these fluctuations with taking moving average, the overall tendency of effective stress reduction quite agree well with the model shown in Figure 6.

The parameter  $w_1$  is given as the total plastic shear work for effective stress ratio of 40 %. Parameter  $S_1$ , the ultimate value is difficult to be discussed since the stress state in the test cannot reach to the ultimate state. Thus,  $S_1$  is given as the most standard empirical value: 0.05. Parameters  $p_1$  and  $p_2$  are given as the value to be most fitted to the measured results by the least square method. Thus, the reduction in effective stress is agreed well with the observation as shown in Figure 8.

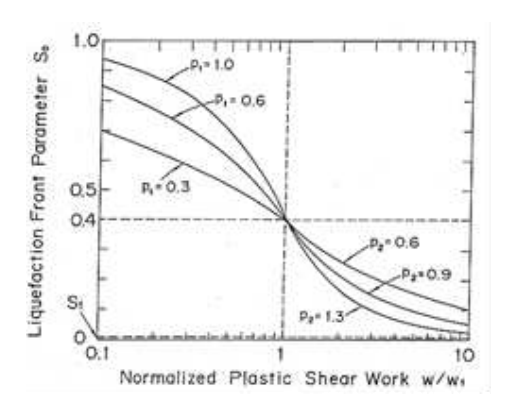


Figure 6. The reduction of effective stress based on plastic shear work (lai et al. 1992)

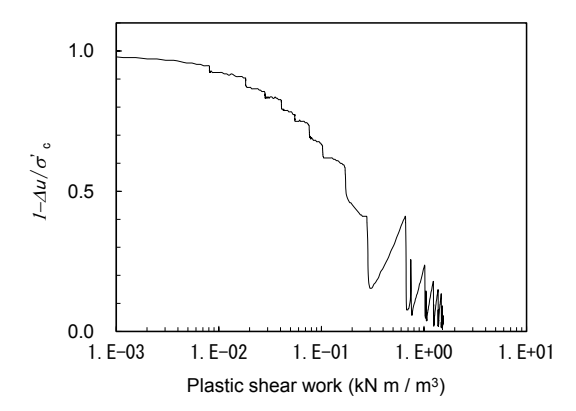


Figure 7. Relationship between the plastic shear work and effective stress ratio in the 8th stage (case 1)

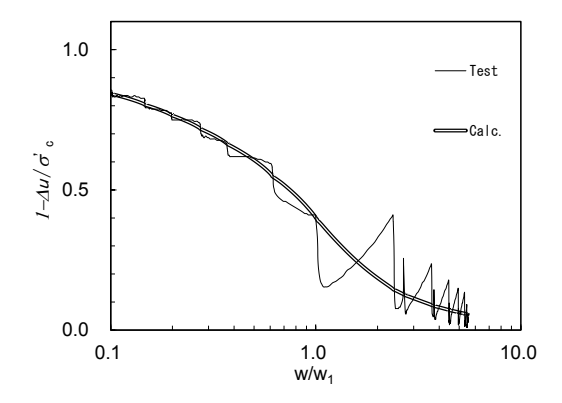


Figure 8. The reduction of effective stress based on plastic shear work (calibrated. Case 1)

# 3.6 Other parameters and summary for all cases

Wet density and the porosity are assumed as 2.0 and 0.471, respectively. Maximum damping factor is given as  $h_{\rm max}$ =0.24. For clean sand, the stress level for the steady state may be a large value, and the parameter  $S_{\rm us}$  is given as zero to ignore the steady state effect.

The parameter identification following the procedure above are conducted for all cases. The summary of the parameters are shown in Table 3.

Table 3 Summary of parameters

Cases	$G_{\mathrm{ma}}$	$\phi$ ' <sub>f</sub>	φ' <sub>p</sub>	$S_{1}$	C 1	W 1	$p_1$	$p_2$
	(kPa)	(deg.)	(deg.)					
Case1	66961	33.8	28.5	0.005	1.40	12.04	0.581	1.193
Case2	54058	34.8	26.7	0.005	1.30	9.14	0.65	1.912
Case3	63005	39.9	23.0	0.005	1.31	11.88	0.4726	0.4937
Case4	64483	44.4	28.9	0.005	1.29	25.21	1.265	0.856

\* G<sub>ma</sub> is the value at confining effective stress of 65.3 kPa

# 4 LIQUEFACTION RESISTANCES

#### 4.1 Liquefaction test simulation

Two series of liquefaction test were conducted for Toyoura sand of Dr = 50 % and 80 %. These liquefaction tests are simulated by single element FEM analyses with the determined parameters shown in Table 3.

The simulation procedure is as follows. First, the element is isotropically consolidated as shown in the first step in Figure 9. Then, cyclic loading of simple shear is applied.

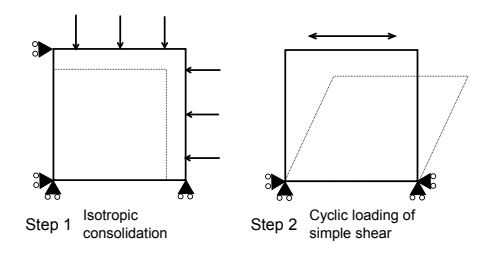


Figure 9. Liquefaction test simulation procedure

# 4.2 Liquefaction resistance curves (Cases of *D*r 50 %)

Liquefaction resistance curves for cases of Dr = 50% are compared in Figure 10. Here, shear strain level of 0.75 %, 1.5 %, 3.75 % in single amplitude and pore water pressure ratio of 95 % are used as the criteria of liquefaction. Focusing on the number of loading cycles of around 10, the liquefaction resistance from the analyses agree well with the test results. However, the liquefaction resistance from analysis does not agree with the test results for the range of loading cycles of 20 or more. The number of loading cycles to cause liquefaction is small for low stress level of loading. This tendency is same with Case 1 and Case 2.

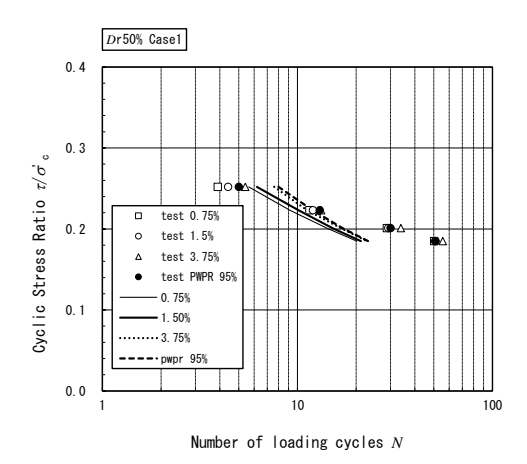
In loose sand case of Dr = 50%, the strain increase rapidly. Thus, the number of loading cycles to gain different strain level are quite similar. This tendency is well simulated in the analysis with the determined parameters.

# 4.3 Liquefaction resistance curves (Cases of *Dr* 80 %)

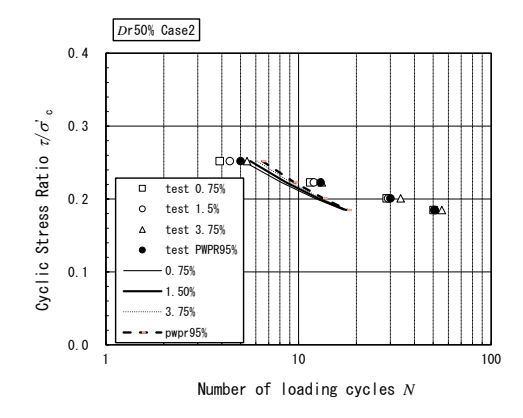
Liquefaction resistance curves for cases of Dr = 80% are compared in Figure 11. The liquefaction resistance curves from the analyses are quite different. Especially, liquefaction resistance is overestimated in Case 3, where

the parameters are determined by stress controlled test. Furthermore, these curves are steeper than the curves of liquefaction test results.

In dense sand case of Dr = 80%, the strain gradually increase. Thus, the number of loading cycles to gain different strain level differs. This tendency is well simulated in the analysis with the determined parameters.



(a) Case 1 (parameters from stress controlled test)



(b) Case 2 (parameters from strain controlled test)

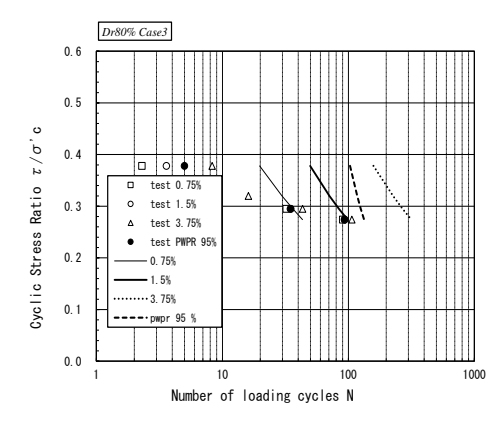
Figure 10. Liquefaction resistance curves for the cases of Dr = 50 % (Case 1 and 2)

# 5 DISCUSSION

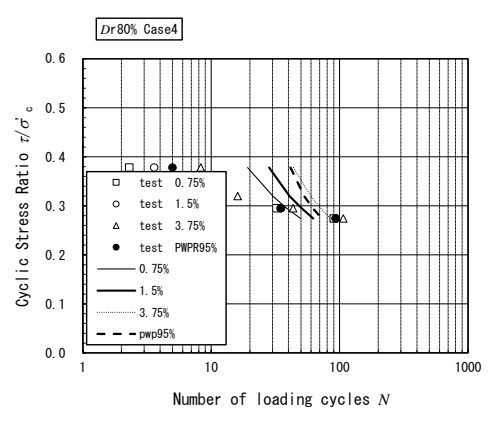
From the comparison of the liquefaction resistance curves from the analysis with the parameters determined by multi-stage cyclic loading test and liquefaction resistance curves from test results, following issues are concerned.

1) The differences of parameters due to the difference of stress/strain controlled tests (Case1/Case2 and Case3/Case4) are summarized in Table 4. The friction angles and parameter  $p_2$  tend to be small for the case using stress-controlled test (Case 2). This is maybe the

underestimation of shear stiffness in Case 2. However, more detailed investigation on the reasons for the differences is necessary. It is important to improve the parameter determination scheme.



(a) Case 3 (parameters from stress controlled test)



(b) Case 4 (parameters from strain controlled test)

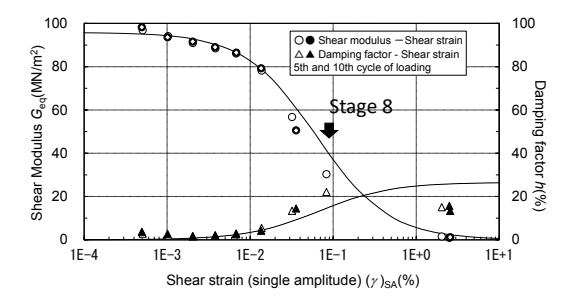
Figure 11. Liquefaction resistance curves for the cases of Dr = 80 % (Case 3 and 4)

2) Focusing on the number of loading cycles of around 10 in Case 1 and Case 2, the liquefaction resistance from the analyses agree well with the test results. However, the liquefaction resistance from analysis does not agree with the test results for the range of loading cycles of 20 or more. This may be because of the parameter setting of  $c_1$ , which corresponds to the threshold stress level. Although the threshold strain level of 0.01 % may be correct, the error of estimated shear modulus may induce the error in the threshold stress level. The shear modulus determined by the 1st half cycle of loading may be rather small, and it may result in the underestimation of  $c_1$ , especially in Case 2.

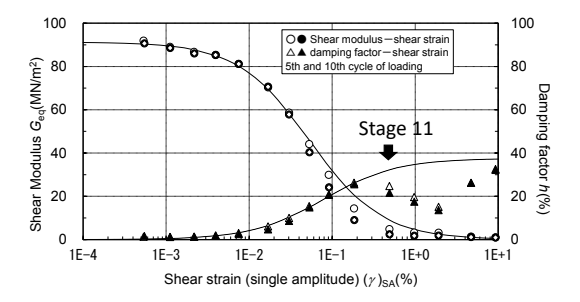
- 3) The proposed Eq. 6 is the equation to give only the lower bound. This is another reason to underestimate parameter  $c_1$ . More adequate scheme to determine the appropriate value of the parameter  $c_1$  is necessary.
- 4) The liquefaction resistances in test results and calculated results are not consistent in Case 3 and Case 4. The difference in Case 3 may be from overestimation of shear stiffness. The difference in Case 4 may be due to other unidentified reasons.
- 5) There is a big difference in the test results in stress controlled test (Case 3) and strain controlled test (Case 4). As shown in Figure 12, there are more number of stages in Case 4, since the control of the strain level is possible in strain controlled test. Therefore, the parameters are determined in Case 3 at stage 8, and in Case 4 at stage 11. It implies the densification of specimen due to drainage between stages affected on the results.
- 6) Effect of the densification due to drainage are examined by the comparison of the relationship between the plastic shear work and residual effective stress. For Case 1, the calibrated curve from the result at stage 8 and the measured relationship at stage 7 are shown in Figure 13. As shown in the figure, the relationships at stage 7 and at stage 8 are different. This may be due to the densification of the specimen, which is observed as the hesitation in decreasing effective stress in later stage. Here, the pore water pressure ratio at stage 7 is about 0.4, as shown in Figure 2 (a). The consideration of the pore water pressure increase in prior stage is an important issue to be considered. Reducing the number of loading stages, reducing the number of loading cycles to prevent the increase in pore water pressure, or proposal of the correction on the effect of densification of the specimen are necessary to avoid the problem related to pore water pressure increase in prior stage.
- 7) The fluctuation of effective stress induced by cyclic mobility is a possible cause of the difference of determined parameter. Figure 14 shows the relationship between the effective stress ratio and plastic shear work in Case 4. The stress state of 40 % of initial effective stress (indicate as a black circle) occur at the bottom of fluctuation. Therefore, the line in the first half (above 40 %) and in the last half (below 40 %) are not connected smoothly at the point indicated as a cericle in the figure. The wrong estimation on the parameter  $w_1$  (given as the plastic shear work at 40 % effective stress) cause consecutive wrong parameter determination in  $p_1$  (related to the curvature in the first half) and p2 (related to the curvature in the last half).

Table 4. Difference of determined parameters for the sand with same relative density

Ratio	$G_{\mathrm{ma}}$	φ' <sub>f</sub>	φ' <sub>p</sub>	<b>c</b> 1	$W_1$	$p_1$	$p_2$
	(kPa)	(deg.)	(deg.)				
Case1/Case2	1.24	0.97	1.07	1.40	1.32	0.89	0.62
$(D_{\Gamma} = 50\%)$							
Case3/Case4	0.98	0.90	0.80	1.02	0.47	0.37	0.58
$(D_{\rm r} = 80\%)$							



(a) Test results in Case 3 (stress controlled)



(b) Test results in Case 4 (strain controlled)

Figure 12. Difference between Case 3 and Case 4

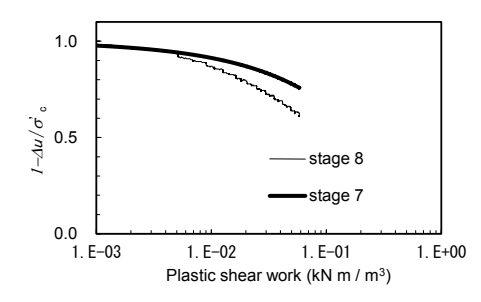


Figure 13. Effect of inter-stage drainage on PWP increase (Case 1: stress controlled test with *D*r = 50 %)

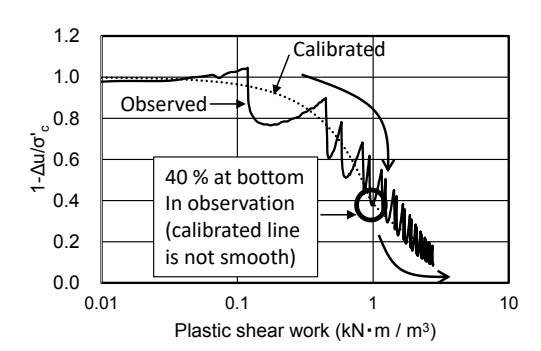


Figure 14. The reduction of effective stress based on plastic shear work (calibrated. Case 4)

# 6 CONCLUSION

In this paper, we challenged parameter calibration of an effective stress analysis from multi-stage cyclic loading test result. We used the test data of a standard multi-stage cyclic loading test as indicated in JGS 0543-2009 "Method for Cyclic Torsional Shear Test on Hollow Cylindrical Specimens to Determine Deformation Properties of Soils", with recording of the pore water pressure during the test. The recorded pore water pressure clarified the drawback of the multi-stage test such as the densification of the specimen due to the drainage between the loading stages.

However, the obtained parameter sets has a certain degree of agreement with the liquefaction test result in terms of strain increase tendency. The rapid increase of strain in loose sand ( $D_{\rm r}$  = 50 %) and gradual increase in dense sand ( $D_{\rm r}$  = 80 %) were successfully simulated with the determined parameter.

The appropriate scheme of the laboratory test may depend on the numerical (constitutive) model used. Since this study used only one model, more trial with various models, such as Cocktail glass model in FLIP ROSE (lai et al., 2011) is necessary as a future study. However, the example of parameter identification in this paper may be a useful reference in the practice, especially in the case with insufficient number of undisturbed in-situ samples to obtain the liquefaction resistance curve.

# **REFERENCES**

Boulanger, R. W., and Ziotopoulou, K. (2015): PM4SAND (version 3): A sand plasticity plane-strain model for earthquake engineering applications, Report No. UCD/CGM-15-01, Center for Geotechnical Modeling, Department of Civil and Environmental Engineering, University of California, Davis, CA, 108p.

Dafalias, Y. F., and Manzari, M. T. (2004): Simple plasticity sand model accounting for fabric change effects, *Journal of Engineering Mechanics*, ASCE, 130(6), pp.622-634.

Fukutake, K., Ohtsuki, A., Sato, M., and Shamoto, Y. (1990): Analysis of saturated dense sand-structure system and comparison with results from shaking

- table test, Earthquake Engineering and Structural Dynamics, 19(7), pp. 977-992.
- Iai, S., Matsunaga, Y., and Kameoka, T. (1992): Strain space plasticity model for cyclic mobility, *Soils and Foundations*, 32(2), pp. 1-15.
- Iai, S., Tobita, T., Ozutsumi, O., and Ueda, K. (2011): Dilatancy of granular materials in a strain space multiple mechanism model. *International Journal for Numerical and Analytical Methods in Geomechanics*, 35(3), pp. 360-392.
- Shnabel, P. B., Lysmer, J., and Seed, H. B. (1972): SHAKE, A computer program for earthquake response analysis of horizontally layers sites, Report No. EERC 72-12, University of California at Berkeley.
- Uemura, K., Ichii, K., Mikami, T. and Ozutsumi, O. (2009): Assessment of liquefaction potential against long duration shaking and its application, *International* Conference on Performance-Based Design in Earthquake Geotechnical Engineering — from case history to practice — (IS-Tokyo'09), Tsukuba, Japan, pp.1477-1482.